

Catalytic Incineration of Acetone on Mesoporous Silica Supported Metal Oxides Prepared by One-Step Aerosol Method

ChenYeh Wang and Hsunling Bai*

Institute of Environmental Engineering, National Chiao Tung University, 1001 University Road, Hsinchu 300, Taiwan

ABSTRACT: Mesoporous silica supported metal oxide catalysts were synthesized by a one-step fast aerosol process based on an evaporation induced self-assembly (EISA) method. They were then applied to the catalytic incineration of VOCs with acetone as the target species. The synthesized metal-MSPs (mesoporous silica particles) were characterized by N₂ adsorption–desorption measurements, X-ray diffraction (XRD), transmission electron microscopy (TEM), and inductively coupled plasma-mass spectrometer (ICP–MS) to understand their physical and chemical properties. Tests on various metals of Ce, Mn, Cu, Fe, and Al supported on MSPs over a temperature range of 150–350 °C demonstrated that Ce is the best metal for the catalytic incineration of acetone. The Ce-MSPs(10) has a high Ce loading of 9.76 wt %, but its small specific surface area of 615 m²/g, poor pore size distribution, and less-ordered pore structure resulted in a relatively lower acetone removal as compared to the Ce-MSPs(25). The Ce-MSPs(25) catalyst appeared to be the best acetone catalytic incineration performance due to the high specific surface area of 951 m²/g with highly ordered pore structure as well as optimal Ce metal content of 3.72 wt % so that CeO₂ particles were well dispersed on the porous surfaces. Near complete acetone destruction via Ce-MSPs(25) catalyst was achieved at a temperature of 250 °C, acetone inlet concentration of 1000 ppmv and GHSV of 5000 h⁻¹. The long-term stability test showed that the acetone destruction efficiency can be kept constant during the 96 h test period.

1. INTRODUCTION

Volatile organic compounds (VOCs) are important air pollutants emitted from many industrial processes. They may pollute the atmosphere, result in photochemical reactions and endanger human health. Among all the VOCs, acetone is a common organic solvent which has been widely used in many industries such as plastics, fibers, drugs, semiconductor, and opto-electronic industries. Thermal oxidation is one of the most efficient technologies to destruct acetone vapors emitted from these industrial plants; however, the direct thermal oxidation process must be maintained at high temperature (>700 °C), and it consumes a lot of energy. Thus catalytic oxidation has attracted wide research attention for VOCs destruction due to its lower working temperature (<500 °C).¹

Noble metal-based catalysts show good activity at low temperatures for the complete oxidation of VOCs.^{2–4} However, the industrial application of noble metal-based catalysts for VOCs destruction is limited by their prices. Thus, there are many different species of transition metals being studied in the literature for catalytic oxidation for VOCs.^{5–7} It has been demonstrated that MnO_x could be effective catalysts for the destruction of VOCs such as toluene.^{5,6} The other study reported that the activity of 5 wt % Cu/γ-Al₂O₃ had a great effect on catalytic oxidation of aromatic hydrocarbons due to the smaller particles and its high dispersion on support.⁷ The Fe–Ti-oxide catalyst exhibited higher activity than Fe₂O₃, pure iron, or titanium oxide and showed a promising catalytic potential for the complete oxidation of chlorobenzene at a relatively low temperature.⁸ The performance of Ce-based catalysts has been tested for the destruction of VOCs compounds because cerium is the most abundant of the lanthanide-based metals and it possesses high oxygen storage capacity.^{9–14}

The hydrophobicity, activity, and pore characteristics of the catalyst support are very important for catalytic combustion.¹⁵ The advantage of using hydrophobic supports was that moistures from atmosphere and oxidation would not be adsorbed on the surface.³ The mesoporous materials such as the MCM-41 was synthesized which possesses hydrophobic property, uniform pore size, and high specific surface area.¹⁶ The hydrophobic mesoporous silica materials have been widely studied on their possible applications for the adsorption^{17,18} or catalytic incineration of VOCs.^{2,10} And it was demonstrated that MCM-41 is better than ZSM-5 due to its high hydrophobicity and pore structure as a catalyst support.⁴

Mesoporous silica particles (MSPs) were modified from the MCM-41 and were synthesized by the evaporation induced self-assembly (EISA) method.¹⁹ The advantage of the aerosol EISA process lies in that it can continuously produce mesoporous silica materials in a very short processing time of a few seconds, which is very fast as compared to the conventional hydrothermal method for producing MCM-41 which requires tens of hours of manufacture time. When used as adsorbents, the volume-based acetone adsorption capacity of MSPs is much higher than that of the MCM-41 and the pressure drop of MSPs are much lower than that of MCM-41.^{20,21}

There have been very limited studies on the preparation of metal-MSPs based on the EISA aerosol spray dried methods because it is a relatively new concept. The MSPs containing Al or Zr were synthesized via the EISA aerosol method,²² and the results

Received: August 29, 2010

Accepted: February 17, 2011

Revised: February 1, 2011

Published: March 02, 2011

Table 1. Physical and Chemical Properties of Metal-MSPs

sample name	Si/Ce ^a molar ratio	Si (wt %)	Ce (wt %)	Si/Ce ^b molar ratio	Vp ^c (cm ³ /g)	S _{BET} ^d (m ² /g)	d _{BJH} ^e (nm)
Ce-MSPs(200)	200	23.67	0.51	232	0.82	1061	2.46
Ce-MSPs(100)	100	26.39	1.19	111	0.81	1033	2.49
Ce-MSPs(50)	50	28.68	1.88	76	0.80	1003	2.54
Ce-MSPs(25)	25	25.32	3.72	34	0.73	951	2.56
Ce-MSPs(10)	10	22.96	9.76	12	0.49	615	2.81
Mn-MSPs(25)	25	31.87	2.72 _{Mn}	23 _{Si/Mn}	0.59	547	3.05
Cu-MSPs(25)	25	30.02	1.48 _{Cu}	46 _{Si/Cu}	0.77	871	2.58
Fe-MSPs(25)	25	30.53	2.71 _{Fe}	22 _{Si/Fe}	0.74	1011	2.59
Al-MSPs(25)	25	25.54	1.34 _{Al}	18 _{Si/Al}	0.74	1020	2.56
MSPs(25)	0				0.90	1153	2.40

^a Si/Ce molar ratio calculated based on the precursor concentration. ^b Actual Si/Ce molar ratio measured by ICP-MS. ^c Pore volume. ^d BET surface area. ^e Pore diameter calculated by BJH theory.

showed that the incorporation of these metals was more hydrothermally stable than pure mesoporous silica. The noble metal incorporated MSPs were synthesized and tested as a catalyst in the hydrodechlorination reaction of 1,2-dichloroethane, and it exhibited near complete conversion and ethylene selectivity at 350 °C.²³ Noble metals of Au were deposited on the MSPs via the amine functionalization method,²⁴ and the Au-NH₂-Co-MSPs showed the highest reactivity for CO oxidation, suggesting that the nature of the support is very important for this reaction.

To prepare the metal oxide catalysts supported on mesoporous silica materials, the conventional hydrothermal method usually requires tedious steps for producing metal oxide catalysts supported on mesoporous silica materials.^{2,4} On the other hand, the one-step synthesis of aerosol EISA method might be a feasible route to produce metal oxide catalysts supported on the mesoporous silica materials. To the authors' knowledge, there is no report available on incorporating the transition metal oxides into the MSPs and applying them to the destruction of VOCs. This study presents results on the physical and chemical characterization of the transition metal-MSPs. And the potential application of the metal-MSPs for the catalytic incineration of acetone, an important VOC emitted from the semiconductor and opto-electronic industries, is demonstrated.

2. EXPERIMENTAL SECTION

2.1. Catalysts Preparation. Five different metals of Ce, Mn, Cu, Fe, and Al were chosen as the metal species because they were widely investigated for the VOCs catalytic destruction studies. The metal precursors were prepared from cerium nitrate, manganese nitrate, copper nitrate, iron nitrate, and aluminum nitrate solutions, respectively. Cetyltrimethylammonium bromide (CTAB) was used as the structure directing template and tetraethoxysilane (TEOS) was used as the silicon precursor. The molar gel composition of the synthesized mixture was 1 SiO₂:0.18 CTAB:10 ethanol:80 H₂O:0.008 HCl:1/X metal. The synthesized samples are denoted as metal-MSPs(X), where X corresponded to the molar ratio of Si/metal in the precursor solution, and it varied from 10 to 200.

All of the precursors were mixed together and stirred for 30 min to obtain a clear solution. The solution was then nebulized by an ultrasonic atomizer (1.8 MHz) with a dry and clean air stream of 2 slpm flow rate and the droplets were passed through two heaters. The first and second heating zones of the aerosol process were controlled at temperatures of 150 and 550 °C,

respectively. The total reaction time of this continuous flow process was approximately 5 s for producing mesoporous silica supported metal oxide catalysts. After reaction, the powders were collected on a filter and calcined at 550 °C for 6 h in air to remove the residual surfactant. Detailed procedures on the EISA aerosol method can be referred to Hung and Bai.²⁰

It was observed that different metals in the MSPs displayed different colors after calcination. The color of pure MSPs was white, while the colors for Mn-MSPs, Cu-MSPs, Fe-MSPs, Al-MSPs, and Ce-MSPs are dark brown, gray, dark red, white, and yellow, respectively.

To verify the performance of the Ce-MSPs catalysts, a Ce-containing catalyst was also made from the commercial ZSM-5 zeolite. The commercial ZSM-5 (CBV5524G, Zeolyst) was calcined at 550 °C for 6 h and then impregnated with cerium nitrate precursor at room temperature under 30 min ultrasonic process. The solution was then dried at 120 °C for 12 h and then calcined at 550 °C for 6 h. The resulting material is marked as Ce-ZSM-5. On the other hand, the Ce/Al-MSPs(X₁/X₂) was synthesized by the one-step aerosol EISA method, where X₁ corresponded to the molar ratio of Si/Ce and X₂ corresponded to the molar ratio of Si/Al in the precursor solution. The molar ratio of Si/Ce and Si/Al for the Ce/Al-MSPs(X₁/X₂) was adjusted to obtain similar metal compositions to those of Ce-ZSM-5.

2.2. Catalysts Characterization. The specific surface area, specific pore volume and BJH pore diameter of the samples were measured by N₂ adsorption-desorption isotherm at 77 K using a surface area analyzer (Micromeritics, ASAP 2020, USA). Prior to the adsorption-desorption measurements, all samples were degassed at 350 °C for 6 h under vacuum pressure of 10⁻⁶ mbar. The elemental metal contents in the catalysts were analyzed by an inductively coupled plasma-mass spectrometer (ICP-MS, SCIEX ELAN 5000). X-ray diffraction (XRD) patterns of calcined samples were recorded by a Rigaku X-ray diffractometer equipped with nickel-filtered CuKα (λ = 1.5405 Å) radiation. The diffraction diagrams of the mesoporous samples were recorded in the 2θ range of low-angles at 2–10° and wide-angles at 10–80° with steps of 0.4° and a count time of 60 s at each point. Transmission electron microscopy (TEM) images of the samples were observed with a JEOL JEM 1210 instrument, before that the samples were ultrasonicated in ethanol and dispersed on carbon film supported on copper grids (200 mesh).

2.3. Catalytic Incineration of Acetone. The oxidation of acetone was carried out by a continuous flow catalytic reactor system. The reactor was a vertical and downward flow reactor

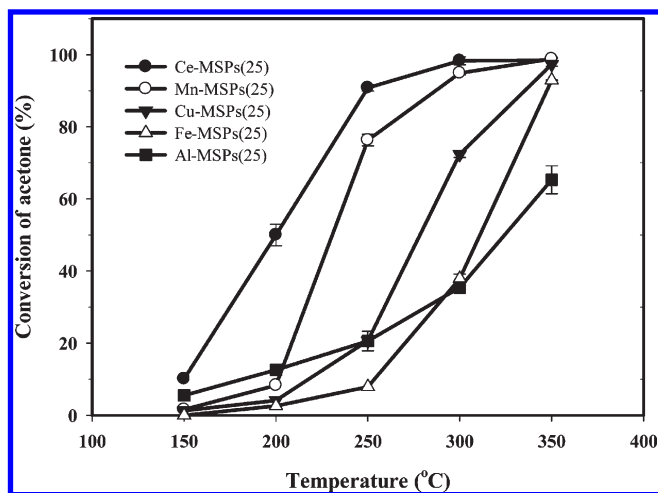


Figure 1. Effect of metal compositions (Ce, Mn, Cu, Fe, Al) on the acetone removal by metal-MSPs. The catalytic incineration tests were obtained under acetone inlet concentration of 1000 ppmv, GHSV of 15000 h⁻¹ and at operation time of 30 min.

made of Pyrex glass tube with 0.8 cm internal diameter. The reactor was heated to the desired temperature with a tubular furnace. Catalysts were tested in 16–30 mesh powdered form and placed in the middle of the glass reactor supported with thin layers of glass wool on both sides. The concentration of acetone was controlled by passing the clean and compressed air through an impinger containing liquid acetone that was kept in a constant temperature-controlled water bath at -10 °C. The total inlet flow rate was controlled to have a GHSV range from 5000 to 15000 h⁻¹ at room temperature (25 °C), which was approached by varying the weight of the catalysts between 0.6 and 0.2 g. The inlet and outlet concentrations of acetone were analyzed by a gas chromatograph (GC 7890A, Agilent) equipped with a flame ionization detector (FID). The removal efficiency of acetone was defined by

$$\text{conversion (\%)} = \frac{I - O}{I} 100$$

where I and O are the inlet and outlet concentrations of acetone, respectively.

3. RESULTS AND DISCUSSION

3.1. Comparison of the Metal-MSPs Catalysts. The chemical and physical properties of metal-MSPs are listed in Table 1. For the Ce-MSPs with Si/Ce precursor molar ratios from 200 to 10, the actual weight percentage of Ce metal ranged from 0.51 to 9.76 wt % as characterized by ICP-MS. An increase in the Ce content led to an increase in the pore size from 2.46 to 2.81 nm. It was observed that all samples indicate evidence of mesopore structure (2 nm < d < 50 nm). But the specific surface areas of all metal-MSPs are smaller than that of the pure MSPs. Because the textural structure of MSPs is similar to that of MCM-41, the decrease trend in the specific surface area by increasing the Ce content in the MSPs is also similar to that of the Ce-MCM-41.^{25,26} And the decrease of pore volume with increasing Ce metal content is also seen in Table 1. For the Si/Ce precursor molar ratio of larger than 25, the specific surface area could still be maintained at 951 m²/g. This indicates that their pore structure was kept in a highly ordered form. For the Ce-MSPs(10), the

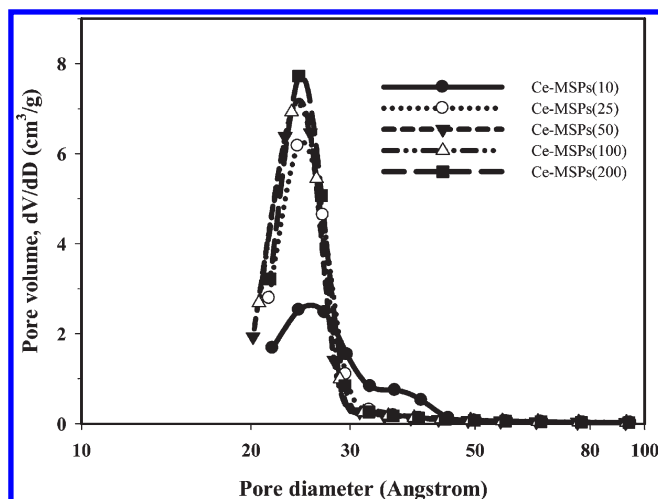


Figure 2. BJH pore size distributions of Ce-MSPs catalysts.

high Ce content of 9.76 wt % in MSPs led to a significant decrease in the specific surface area to only 615 m²/g; this revealed possible collapse of their pore structure.

At the same Si/metal content of 25, all metal-MSPs had the same pore size of 2.56–2.59 nm except for the Mn-MSPs(25) whose pore size was 3.05 nm. And the specific surface area of Mn-MSPs(25) is also much less than those of other metal-MSPs(25). Among all tested metals, the specific surface areas of Fe-MSPs(25) and Al-MSPs(25) appeared to be less affected by the metals incorporated into the mesoporous silica materials.

The catalytic oxidation performances of acetone using Ce, Mn, Cu, Fe, and Al supported MSPs catalysts were compared to obtain the best metal oxide for the acetone destruction. The acetone removal of these five metal-MSPs catalysts are demonstrated in Figure 1 as a function of temperature. It appeared that Ce was the most active metal at the temperature range of 150–350 °C as compared to other metals. The T90 (temperature at which 90% removal was achieved) for the acetone removals were roughly at 250, 300, 350, and 350 °C, respectively, for Ce-MSPs(25), Mn-MSPs(25), Cu-MSPs(25), and Fe-MSPs(25). On the other hand, the acetone removal for Al-MSPs(25) was only 65% even at 350 °C. The results were similar to literature studies^{12,14} which demonstrated that the reactivity of CeO₂ was better than those of Mn₂O₃, CuO, Fe₂O₃, and Al₂O₃ for the destruction of naphthalene and toluene compounds, respectively. However there are also literature studies^{5,6} which indicated the high performance of using Mn-containing oxides as the active metal species. In this study, the reactivity of Mn-MSPs is only second to that of the Ce-MSPs(25), this may be because the Mn-MSPs have the lowest specific surface area of 547 m²/g, which is much less than that of the Ce-MSPs(25), 951 m²/g. Besides, the generation of MnO_x particles on the surface of mesoporous silica material instead of doping into the pore structure may also influence the surface area. Further studies must be conducted to clarify the metal activities of Mn and Ce oxides.

In the following study, the catalyst characterization and the acetone removal efficiency will be focused on the Ce-MSPs of various metal contents.

3.2. Characterization of the Ce-MSPs Catalysts. Figure 2 shows the pore size distribution curves for the Ce-MSPs. The BJH pore size distributions of all samples except Ce-MSPs(10)

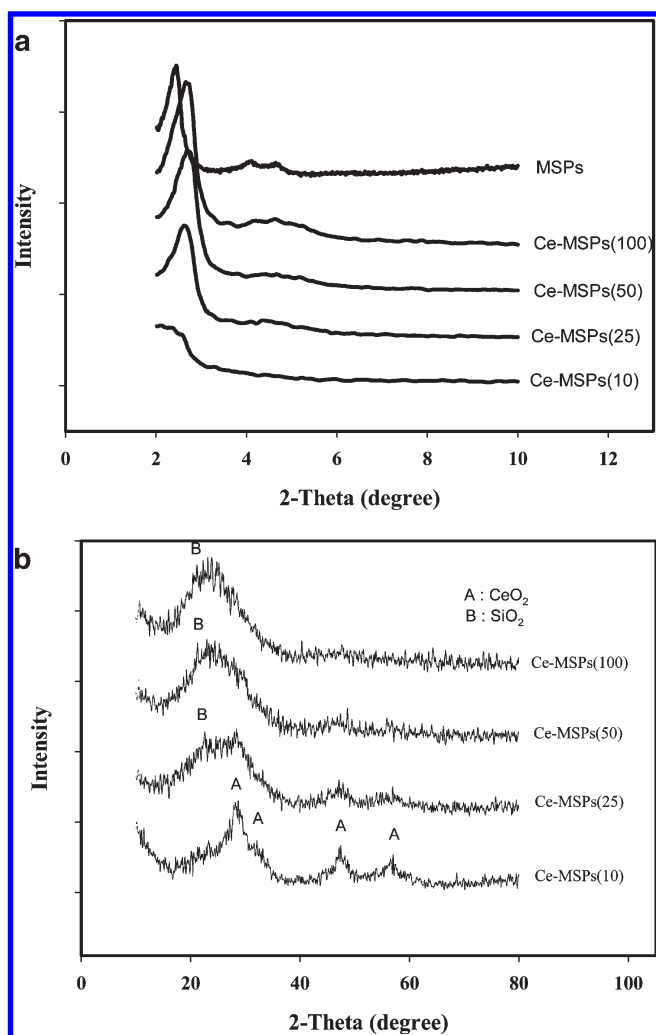


Figure 3. (a) Low-angle and (b) wide-angle X-ray diffraction patterns of catalysts: Ce-MSPs(10); Ce-MSPs(25); Ce-MSPs(50); Ce-MSPs(100).

displayed narrow pore size distribution. Increasing the Ce metal content in the MSPs led to decreases in the pore volume of the peak size. This indicated that their uniform mesoporous structure was decreasing. And Ce-MSPs(10) showed the poorest pore size distribution with an additional peak mode at 30–40 Å, it indicated partial loss of ordered pore size arrangement. It is also possible that the Cerium oxide particles were presented as agglomerated particles and resulted in interparticle pores.

Low-angle ($2 \leq 2\theta \leq 10^\circ$) X-ray diffraction patterns of the Ce-MSPs are depicted in Figure 3a. The (100) diffraction peaks located at about $2\theta=2.3\text{--}2.7^\circ$ were clearly observed for all samples. This revealed the evidence of mesoporous structure.^{20,27} The shape of the XRD peak became flat and the intensity was smaller as the Ce content was increased. This result is similar to those of mesoporous silica particles containing Al or Zr which suggested the loss of long-range order.²² The presence of broadening and reduction in the intensity of diffraction peak for Ce-MSPs(10) confirms the collapse of some pores and thus led to the less-ordered mesoporous structure and smaller surface area as well.

Figure 3b shows the results of wide-angle ($10^\circ \leq 2\theta \leq 80^\circ$) XRD patterns of Ce-MSPs. The peak at about 23° was due to the amorphous silica.²³ The broad diffraction lines due to the CeO₂

(PDF-ICDD 34-0394) were seen, and the characteristic diffraction peaks of CeO₂ structure are at $2\theta = 28.8, 33.3, 47.5$ and 56.4° .^{11,28} The XRD patterns exhibited poor crystalline of CeO₂ in Figure 3b; the results are similar to the CeO₂–SiO₂ which calcined at 773 K.²⁹ It is clearly seen that more Ce content exhibited more intensity of the CeO₂ diffraction peak and less intensity of the amorphous SiO₂ diffraction peak. Among these catalysts, Ce-MSPs(10) had the largest number of CeO₂ structures which indicated a poor distribution of CeO₂ on the surface of the catalyst. The CeO₂ in Ce-MSP catalysts may be presented in larger particle sizes or in agglomeration form. On the other hand, a decrease in the Ce content led to a decrease in the CeO₂ intensity for the Ce-MSPs samples, and the Ce content of 1.19 wt % for Ce-MSPs(100) exhibited no observable XRD peak of CeO₂. This could be because the small amount of CeO₂ could be uniformly distributed and the size of CeO₂ particles was below the detection limit of the XRD instrument.

The TEM images of pure MSPs and Ce-MSPs are shown in Figure 4. One can see in Figure 4a that, for the pure MSPs without loading any metals, the hexagonal pores were clearly seen with highly ordered arrangement. Increasing Ce loading resulted in a more clear observation of the cerium particles, and for the Ce-MSPs(10) which loaded with 9.76 wt % of Ce, the ordered pore structure seemed to be partial collapsed. This was in accord with the surface area data shown in Table 1 and the XRD pattern shown in Figure 3a. The CeO₂ particles appeared to be well dispersed on the surface of the MSPs as clearly seen in Figure 4c for Ce-MSP(25). However, there was also a possibility of encapsulating the CeO₂ particles in the pores of MSPs, thus the pore diameter (d_{BJH}) of the Ce-MSPs was slightly enlarged as seen in Table 1.

3.3. Catalytic Incineration of Acetone by Ce-MSPs. Except stated otherwise, results of all catalytic incineration tests were shown under the base condition of acetone inlet concentration of 1000 ppmv, GHSV of 15000 h^{-1} , and at operation time of 30 min.

Figure 5 presents the relationship between Ce loaded amount of Ce-MSPs and their corresponding acetone removals and specific surface area at the reaction temperature of 250 °C. The experimental results indicated that the Ce-MSPs(25), of which the BET surface area was $951 \text{ m}^2/\text{g}$ and Ce metal content was 3.72 wt %, appeared to have the best acetone catalytic incineration performance, and the worst acetone removal was Ce-MSPs(200), which had the highest BET surface area of $1061 \text{ m}^2/\text{g}$, but the lowest Ce metal content of 0.51 wt %. Increasing the metal content in the catalysts would provide more active sites and result in increasing the reaction probability of the catalysts with acetone molecules for Ce content up to 3.72 wt %. A further increase of Ce content to 9.76 wt % (Ce-MSPs(10)) resulted in slightly decreases in the acetone removal. The optimal Ce amount of 3.72 wt % loaded on the MSPs is much less than the metal loading amounts of 10–20 wt % typically used in the literature for the postloading process of metals onto zeolites,³⁰ MCM-41 mesoporous silica materials,³¹ or $\gamma\text{-Al}_2\text{O}_3$ ³² supports. This is because the amount of metals would affect both the physical and chemical properties of the metal catalysts during the one-step synthesis of the Ce-MSPs. On the Ce-MSPs(25), the highly ordered mesoporous structure of MSPs support could be maintained while the CeO₂ active metal was well dispersed.

The influence of space velocity on the catalytic performance was examined over the Ce-MSPs(25) catalyst and the result was shown in Figure 6. It was observed that space velocity has a significant influence at temperatures below 250 °C. A near complete removal

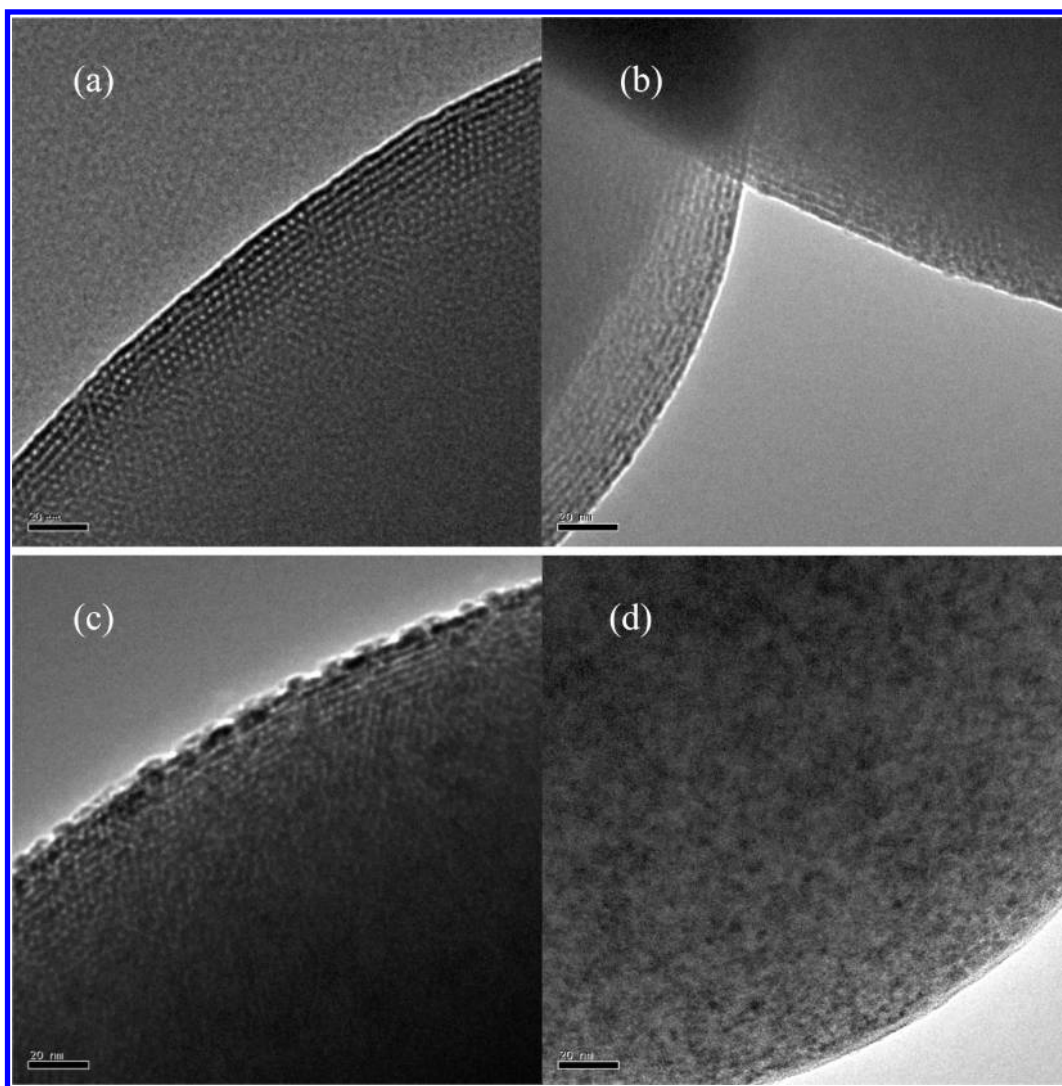


Figure 4. TEM images of calcined mesoporous materials: (a) MSPs; (b) Ce-MSPs(50); (c) Ce-MSPs(25); (d) Ce-MSPs(10); all images have the same scale bar of 20 nm.

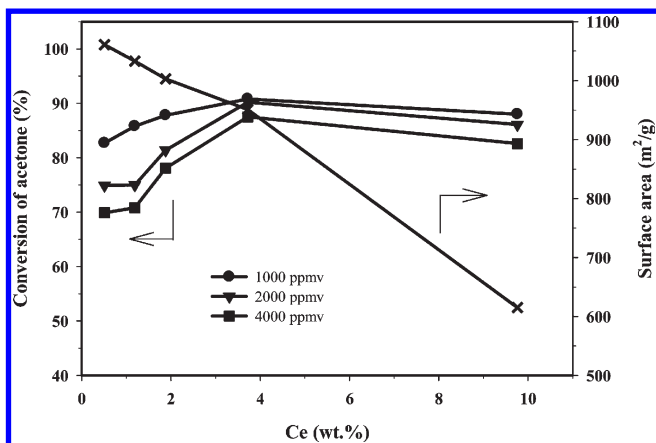


Figure 5. The correlation between acetone removal, specific surface area, and Ce-loaded content for Ce-MSPs at a temperature of 250 °C.

of acetone is achievable at 250 °C for Ce-MSPs(25) at GHSV of 5000 h⁻¹. But for GHSV of 15000 h⁻¹ the complete removal would be achieved at a higher temperature of 300 °C.

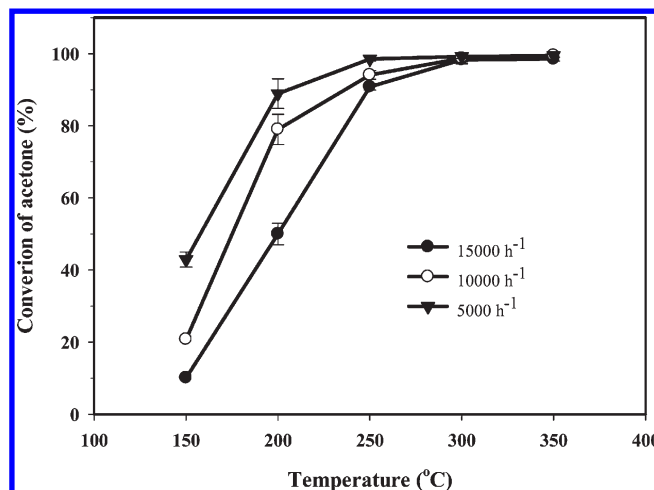


Figure 6. Effect of GHSV on the acetone removal of Ce-MSPs(25).

The stability of Ce-MSPs(25) was tested for 96 h under acetone concentration of 4000 ppmv, reaction temperature of

Table 2. Physical and Chemical Properties of Ce/Al-MSPs(50/25) and Ce-ZSM-5

sample name	Si ^a (wt %)	Ce ^a (wt %)	Al ^a (wt %)	V _p ^b (cm ³ /g)	S _{BET} ^c (m ² /g)	d _{BJH} ^d (nm)
Ce/Al-MSPs(50/25)	33.07	2.74	1.18	0.71	917	2.53
Ce-ZSM-5	30.72	2.75	1.21	0.16	384	6.66

^a Actual Si (wt %), Ce (wt %), and Al (wt %) measured by ICP-MS. ^b Pore volume. ^c BET surface area. ^d Pore diameter calculated by BJH theory.

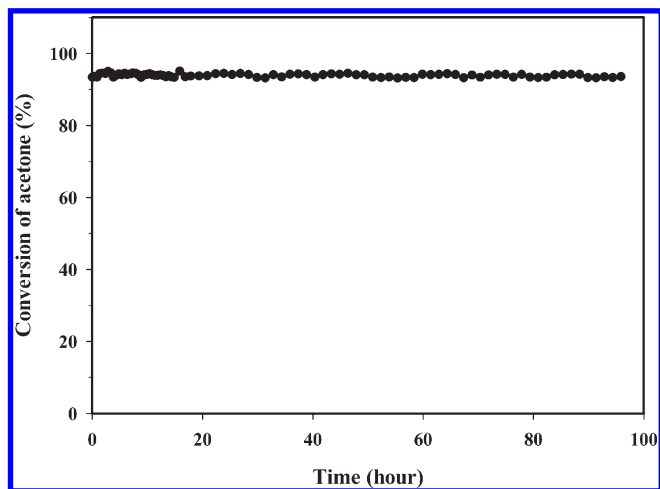


Figure 7. Acetone removal as a function of time-on-steam for acetone concentration = 4000 ppmv, GHSV = 5000 h⁻¹, and operation temperature of 250 °C on Ce-MSPs(25) catalyst.

250 °C, and GHSV of 5000 h⁻¹. The result is depicted in Figure 7. The Ce-MSPs(25) catalyst showed very stable activity for 96 h, the acetone removal efficiency can be kept at around 93% during the test period. The superiority of active metals supported on mesoporous materials over various zeolite materials were also observed on the SBA-15² and the MCM-41^{31,33} mesoporous materials. This could be because the mesoporous silica materials have weaker and less acid sites so that the coke formation is limited.² This may also be the reason for the long-term stability of the Ce-MSPs(25) catalyst used in this study.

3.4. Comparison with ZSM-5-Based Catalyst. To further explore the performance of the Ce-MSPs catalysts, the commercial ZSM-5 zeolite was impregnated with the same cerium metal precursor solution to obtain a zeolite-based catalyst. Because the Ce-ZSM-5 zeolite catalyst was composed of Si, Al, and Ce metals, the Ce/Al-MSPs catalyst was also manufactured to have similar composition to that of the Ce-ZSM-5 catalyst, and its physical and chemical properties are shown in Table 2. One can see that both of the Ce/Al-MSPs(50/25) and Ce-ZSM-5 catalysts had almost the same Ce and Al metal contents as characterized by ICP-MS. The major difference between the two catalysts was their pore structures. For example, Ce/Al-MSPs(50/25) made from the one-step aerosol process had a higher specific surface area of 917 m²/g as compared to the Ce-ZSM-5, which had a lower surface area of only 384 m²/g. Figure 8 compared the acetone removal efficiencies of Ce/Al-MSPs(50/25) and Ce-ZSM-5 at a low operation temperature of 200 °C. It was observed that the acetone conversion was 85% using the meso-structured Ce/Al-MSPs(50/25), which is higher than the 76% acetone conversion of the Ce-ZSM-5. This indicated that the one step aerosol EISA method can produce better metallic Ce/Al-MSPs catalyst than commercial Ce-ZSM-5 catalyst in terms of acetone conversion performance.

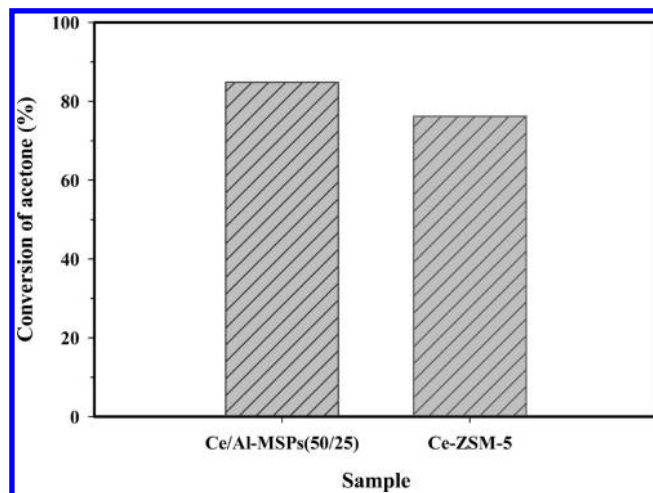


Figure 8. Comparison on the acetone removal efficiency between Ce-MSPs and Ce-ZSM-5 zeolite catalysts at the operation temperature of 200 °C.

4. CONCLUSIONS

Metal oxides supported on the mesoporous silica materials were successfully synthesized by the one step aerosol EISA method and applied to the acetone destruction. Unlike conventional hydrothermal processes which required tedious steps for manufacturing metal oxides catalysts supported on mesoporous silica materials, the one-step aerosol EISA process has the advantage of time-saving and can be designed as a continuous process for easy mass production. The CeO₂ was the most active metal species as compared to Mn, Cu, Fe, Al of the same precursor amounts supported on MSPs for the catalytic incineration of acetone. Among the five different Ce loading amounts, Ce-MSPs(25) shows the best catalytic activity due to its relatively high BET surface area of 951 m²/g and optimal Ce metal content of 3.72 wt %. This yields the catalyst properties of highly ordered mesoporous structure with well-dispersed CeO₂ particles which provides easier contact of acetone vapors with the active metal species. At a temperature of 250 °C, the acetone destruction efficiency can be completed at an acetone inlet concentration of 1000 ppmv and GHSV of 5000 h⁻¹. And the catalytic incineration performance can be maintained stable within 96 h test period. The acetone removal performance of bimetallic Ce/Al-MSPs(50/25) and Ce-ZSM-5 at a low temperature of 200 °C was greatly better than the monometallic Ce-MSPs and Al-MSPs catalysts. And the acetone removal performance of Ce/Al-MSPs(50/25) (synthesized by one step aerosol EISA method) was better than the commercial Ce-ZSM-5 catalyst under almost the same metal content.

■ AUTHOR INFORMATION

Corresponding Author

*Tel.: +886-3-573-1868. Fax: +886-3-572-5958. E-mail: hlbai@mail.nctu.edu.tw.

ACKNOWLEDGMENT

The authors gratefully acknowledge the financial support from the National Science Council of Taiwan under Contract Number NSC97-2628-E-009-025-MY2.

REFERENCES

- (1) Khan, F. I.; Ghoshal, A. K. Removal of Volatile Organic Compounds from Polluted Air. *J. Loss Prevent. Process Ind.* **2000**, *13*, 527.
- (2) He, C.; Li, J.; Cheng, J.; Li, L.; Li, P.; Hao, Z.; Xu, Z. P. Comparative Studies on Porous Material-Supported Pd Catalysts for Catalytic Oxidation of Benzene, Toluene, and Ethyl Acetate. *Ind. Eng. Chem. Res.* **2009**, *48*, 6930.
- (3) Wu, J. C. S.; Chang, T. Y. VOC Deep Oxidation over Pt Catalysts Using Hydrophobic Supports. *Catal. Today* **1998**, *44*, 111.
- (4) Xia, Q. H.; Hidajat, K.; Kawi, S. Adsorption and Catalytic Combustion of Aromatics on Platinum-Supported MCM-41 Materials. *Catal. Today* **2001**, *68*, 255.
- (5) Li, W. B.; Chu, W. B.; Zhuang, M.; Hua, J. Catalytic Oxidation of Toluene on Mn-Containing Mixed Oxides Prepared in Reverse Microemulsions. *Catal. Today* **2004**, *93–95*, 205.
- (6) Agüero, F. N.; Barbero, B. P.; Sanz, O.; Lozano, F. J. E.; Montes, M.; Cadús, L. E. Influence of the Support on MnO_x Metallic Monoliths for the Combustion of Volatile Organic Compounds. *Ind. Eng. Chem. Res.* **2010**, *49*, 1663.
- (7) Kim, S. C. The Catalytic Oxidation of Aromatic Hydrocarbons over Supported Metal Oxide. *J. Hazard. Mater.* **2002**, *B91*, 285.
- (8) Khaleel, A.; Al-Nayli, A. Supported and Mixed Oxide Catalysts Based on Iron and Titanium for the Oxidative Decomposition of Chlorobenzene. *Appl. Catal. B* **2008**, *80*, 176.
- (9) Angel, G. D.; Padilla, J. M.; Cuauhtemoc, I.; Navarrete, J. Toluene Combustion on γ -Al₂O₃-CeO₂ Catalysts Prepared from Boehmite and Cerium Nitrate. *J. Mol. Catal. A: Chem.* **2008**, *281*, 173.
- (10) Araujo, A. S.; Aquino, J. M. F. B.; Souza, M. J. B.; Silva, A. O. S. Synthesis, Characterization and Catalytic Application of Cerium-Modified MCM-41. *J. Solid State Chem.* **2003**, *171*, 371.
- (11) Dai, Q.; Wang, X.; Lu, G. Low-Temperature Catalytic Combustion of Trichloroethylene over Cerium Oxide and Catalyst Deactivation. *Appl. Catal. B* **2008**, *81*, 192.
- (12) Garcia, T.; Solsona, B.; Taylor, S. H. Naphthalene Total Oxidation over Metal Oxide Catalysts. *Appl. Catal. B* **2006**, *66*, 92.
- (13) Gutierrez-Ortiz, J. I.; Rivas, B.; Lopez-Fonseca, R.; Gonzalez-Velasco, R. Study of the Temperature-Programmed Oxidative Degradation of Hydrocarbons over Ce-Based Catalysts by Evolved Gas Analysis. *J. Therm. Anal. Calorim.* **2007**, *87*, 55.
- (14) Wang, C. H.; Lin, S. S. Preparing an Active Cerium Oxide Catalyst for the Catalytic Incineration of Aromatic Hydrocarbons. *Appl. Catal. A* **2004**, *268*, 227.
- (15) Li, W. B.; Wang, J. X.; Gong, H. Catalytic Combustion of VOCs on Non-noble Metal Catalysts. *Catal. Today* **2009**, *148*, 81.
- (16) Beck, J. S.; Vartull, J. C.; Roth, W. J.; Leonowicz, M. E.; Kresge, C. T.; Schmitt, K. D.; Chu, C. T. W.; Olson, D. H.; Sheppard, E. W.; McCullen, S. B.; Higgins, J. B.; Schlenker, J. L. A New Family of Mesoporous Molecular Sieves Prepared with Liquid Crystal Templates. *J. Am. Chem. Soc.* **1992**, *114*, 10834.
- (17) Ghiaci, M.; Abbaspur, A.; Kia, R.; Seyedejn-Azad, F. Equilibrium Isotherm Studies for the Sorption of Benzene, Toluene, and Phenol onto Organo-zeolites and as-Synthesized MCM-41. *Sep. Purif. Technol.* **2004**, *40*, 217.
- (18) Zhao, X. S.; Ma, Q.; Lu, G. Q. VOC Removal: Comparison of MCM-41 with Hydrophobic Zeolites and Activated Carbon. *Energy Fuels* **1998**, *12*, 1051.
- (19) Lu, Y.; Fan, H.; Stump, A.; Ward, T. L.; Rieker, T.; Brinker, C. J. Aerosol-Assisted Self-Assembly of Mesoporous Spherical Nanoparticles. *Nature* **1999**, *398*, 223.
- (20) Hung, C. T.; Bai, H. L. Adsorption Behaviors of Organic Vapors Using Mesoporous Silica Particles Made by Evaporation Induced Self-Assembly Method. *Chem. Eng. Sci.* **2008**, *63*, 1997.
- (21) Hung, C. T.; Bai, H. L.; Karthik, M. Ordered Mesoporous Silica Particles and Si-MCM-41 for the Adsorption of Acetone: A Comparative Study. *Sep. Purif. Technol.* **2009**, *64*, 265.
- (22) Bore, M. T.; Marzke, R. F.; Ward, T. L.; Datye, A. K. Aerosol Synthesized Mesoporous Silica Containing High Loading of Alumina and Zirconia. *J. Mater. Chem.* **2005**, *15*, 5022.
- (23) Hampsey, J. E.; Arsenaault, S.; Hu, Q.; Lu, Y. One-Step Synthesis of Mesoporous Metal-SiO₂ Particles by an Aerosol-Assisted Self-Assembly Process. *Chem. Mater.* **2005**, *17*, 2475.
- (24) Bore, M. T.; Mokhonoana, M. P.; Ward, T. L.; Coville, N. J.; Datye, A. K. Synthesis and Reactivity of Gold Nanoparticles Supported on Transition Metal Doped Mesoporous Silica. *Microporous Mesoporous Mater.* **2006**, *95*, 118.
- (25) Kadgaonkar, M. D.; Laha, S. C.; Pandey, R. K.; Kumar, P.; Mirajkar, S. P.; Kumar, R. Cerium-Containing MCM-41 Materials as Selective Acylation and Alkylation Catalysts. *Catal. Today* **2004**, *97*, 225.
- (26) Laha, S. C.; Mukherjee, P.; Sainkar, S. R.; Kumar, R. Cerium Containing MCM-41-type Mesoporous Materials and Their Acidic and Redox Catalytic Properties. *J. Catal.* **2002**, *207*, 213.
- (27) Park, S. H.; Song, B. Y.; Lee, T. G. Effects of Surfactant/Silica and Silica/Cerium Ratios on the Characteristics of Mesoporous Ce-MCM-41. *J. Ind. Eng. Chem.* **2008**, *14*, 261.
- (28) Mu, Z.; Li, J. J.; Tian, H.; Hao, Z. P.; Qiao, S. Z. Synthesis of Mesoporous Co/Ce-SBA-15 Materials and Their Catalytic Performance in the Catalytic Oxidation of Benzene. *Mater. Res. Bull.* **2008**, *43*, 2599.
- (29) Reddy, B. M.; Khan, A.; Lakshmanan, P. Structural Characterization of Nanosized CeO₂-SiO₂, CeO₂-TiO₂, and CeO₂-ZrO₂ Catalysts by XRD, Raman, and HREM Techniques. *J. Phys. Chem. B* **2005**, *109*, 3355.
- (30) Barman, S.; Pradhan, N. C.; Basu, J. K. Kinetics of Alkylation of Benzene with Isopropyl Alcohol over Ce-Exchanged NaX Zeolite. *Ind. Eng. Chem. Res.* **2005**, *44*, 7313.
- (31) Li, W. B.; Zhuang, M.; Xiao, T. C.; Green, M. L. H. MCM-41 Supported Cu-Mn Catalysts for Catalytic Oxidation of Toluene at Low Temperatures. *J. Phys. Chem. B* **2006**, *110*, 21568.
- (32) Kim, H. J.; Choi, S. W.; Inyang, H. I. Catalytic Oxidation of Toluene in Contaminant Emission Control Systems Using Mn-Ce/ γ -Al₂O₃. *Environ. Technol.* **2008**, *29*, 559.
- (33) Karthik, M.; Lin, L. Y.; Bai, H. L. Bifunctional Mesoporous Cu-Al-MCM-41 Materials for the Simultaneous Catalytic Abatement of NO_x and VOCs. *Microporous Mesoporous Mater.* **2009**, *117*, 153.